FLUID FLOW CHRACTERICTICS ON SCALE DEPOSITION IN A CONCENTRIC REDUCER USING CFD APPROACH

Prasanjit Das[1]*, Khan, M.M.K.[1], M.G. Rasul[1] and Suvash C. Saha[2]
[1*]School of Engineering and Technology, Central Queensland University, QLD 4702, Australia
[2] Faculty of Science and Engineering, School of Chemistry, Physics and Mechanical Engineering, Queensland University of Technology, QLD 4001, Australia
Email: p.das@cqu.edu.au

ABSTRACT

Fluid flow phenomenon in a concentric reducer is modelled by computational Fluid Dynamics (CFD) approach to examine the role of fluid velocity in scale formation. Scale formation in alumina refineries is a common phenomenon and it occurs where supersaturated solutions are in contact with solid surfaces. It often leads to serious on-going technical problems and is a major cause of production loss due to equipment downtime required for descaling and cleaning operations. The scale formation mechanism in Bayer process equipment is complex and is not yet fully understood. Numerous researchers indicate that scale growth is strongly affected by fluid velocity while also influenced by a number of other factors such as the quality of bauxite ore, rheological properties of fluid, turbulence and inertia of suspended particles and adhesive property of particles. A numerical study using the Finite Volume Method to analyse the fluid dynamics behaviour of water as it flows through a concentric reducer commonly used in the Bayer plant is presented. The simulation results show a significant variation of the stream-wise (u_x') and cross-stream (u_r') components of the fluctuating velocity as flow passes through the concentric reducer.

INTRODUCTION

Scale formation in pipe work and process equipment is inherent to the operation of many mineral process industry. Scale formation in the Bayer process equipment is a natural consequence of supersaturated solutions that are generated throughout the process. The scale formation problem has a particular significance to alumina refineries where supersaturated solutions rapidly deposit scale in many areas of the Bayer process. The concurrent dissolution of impurities, primarily silica containing materials that originate from the bauxite ore, can result in scale forming in various parts of the process plant. The accumulation of scale reduces the production efficiency considerably and causes other problems such as pipe blockage, probe malfunction, reduction in heat exchanger efficiency and operational costs involved in the de-scaling process. At different stages in the alumina refining process the formation of scale may be rapid; taking merely week to completely block process equipment, or it may form progressively over many months.

NOMENCLATURE

τ_p	[s]	Particle relaxation time (s)
τ_e	[s]	Lifetime of smallest eddies; Kolmogorov time scale of fluctuations based on the volume-averaged viscous energy dissipation (s)
τ_p^+	[-]	Dimensionless particle relaxation time
d_p	[mm]	Particle velocity
ρ_f	[kg m^{-3}]	Density of fluid
ν_f	[m^2 s^{-1}]	Kinematic viscosity of fluid
ρ_p	[kg m^{-3}]	Density of particle
$u*$	[m s^{-1}]	Friction velocity
τ_w	[kg m^{-1} s^{-2}]	Wall shear stress
U_0	[m s^{-1}]	Mean flow velocity\
f	[-]	Friction factor (American)
u_r	[m s^{-1}]	Cross-stream component of instantaneous velocity
$\overline{u}_r$	[m s^{-1}]	Cross-stream component of instantaneous velocity
u_r'	[m s^{-1}]	Fluctuating component of cross-stream velocity
$\sqrt{(u_r')^2}$	[m s^{-1}]	Root-mean-square of the fluctuating cross-stream velocity
$\overline{u}_x$	[m s^{-1}]	Time-averaged value of the stream-wise velocity component
u_x'	[m s^{-1}]	Fluctuating component of stream-wise velocity
$\sqrt{(u_x')^2}$	[m s^{-1}]	Root-mean-square of the fluctuating stream-wise velocity

One of the focus areas of an alumina refinery that is the most susceptible to rapid scale formation is the precipitation area, where hydrargillite precipitates from the supersaturated caustic aluminate solution in which it is dissolved. As well as precipitating into the crystalline gibbsite form to be later separated from the solution, the gibbsite also deposits onto the surfaces that the supersaturated solution contacts. This

formation of scale in the gibbsite dissolution process contributes to more than half [2] of the scaling-related issues experienced in the alumina refinery process. Establishing mechanisms to inhibit scale growth, particularly in the precipitation area of the Bayer process, has long been the subject of significant interest and research. In recent years, this interest has increased as improving plant efficiency and equipment utilisation has become critical to sustaining low-cost alumina production. In order to improve the efficiency of the gibbsite precipitation process through reduced scale deposition on process plant and equipment, fundamental research has been necessary to understand firstly, the mechanisms which facilitate the mechanical bonding to and growth of the scale on equipment surfaces; and thirdly fluid dynamics and fluid's rheology in scale formation.

Here, fundamentals of scale suppression mechanisms from the perception of fluid dynamics are discussed. Very limited work has been conducted on scale formation mechanisms in slurry pipes and slurry tanks used in minerals processing industries such as aluminium refineries. In the extensive literature, most of the topics are related to fouling in evaporators [3], membranes used in the reserve osmosis processes in desalination plants [4] and heat exchangers [5]. Loan *et al.* in CSIRO (*Commonwealth Scientific and Industrial Research Organisation),* experimentally investigated scale formation in slurry tanks by X-ray photoelectron spectroscopy and they observed that, at the initial stage, scale is formed as a result of precipitation reactions other than solids settling [6]. Many researchers [1, 3, 7, 8] suggest that scale growth in the processing equipment is affected by a number of factors including supersaturation in solution, phase transformation, run time, form of material surfaces and flow characteristics (velocity, flow rate and Reynolds number). In the chemical industry, slurry mixing tank agitators are often designed on the basis of achieving off-bottom suspension to resist the settle time for crystallisation [9-11]. In this case, axial flow impellers pumping downward with vertical baffles are more energy efficient than radial turbines [9-11] and the energy efficiency for off-bottom solids suspension is sensitive to impeller off-bottom clearance and impeller diameter [12-18].

A condition of what is considered the successful operation of a precipitation tank is the minimised growth of scale on the wall and cone region of a typical gibbsite alumina precipitation tank at QAL (Queensland Aluminium Limited). It has been identified through operational experience that the rate of scale formation and growth is, in the part, a function of the relative velocity of the supersaturated caustic-aluminate solution on the tank wall.

A collaborative research program was commenced in 1996 between QAL and CSIRO Advanced Fluid Dynamics Laboratory (Melbourne, Australia) to explore a new agitation system for precipitation tanks at QAL. Preliminary research demonstrated that the flow regime developed by the new mechanical agitators was significantly different to that obtained from the more common axial flow rotor with draft tube or air agitated tanks. A novel scale-velocity model was developed [14] for elucidation the scale growth and suppression in an alumina refinery. In this model, a relationship between the fluid flow velocity and scale formation is schematically illustrated in Figure 1. There are four regimes recognized to understand the scale growth mechanism, namely (A) mass transfer control, (B) chemical reaction control, (C) suppression by erosion and (D) erosion damage.

In regime A, the initial scale is negligible at zero velocity as followed by molecular diffusion-rate controlled process. Then the scale growth rate starts very speedily as fluid velocity increases owing to an increase effect of mass transfer. This elucidation is strongly supported by the study of Hoang *et al.* [7] that the increase in gypsum scale growth rate with increasing fluid velocity in a range from 0 to 0.07 m/s.

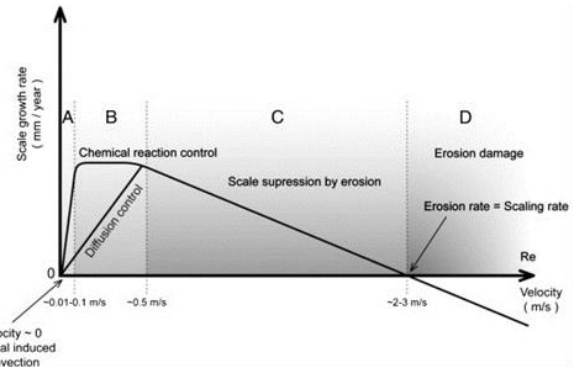

Figure 1 Relationship between the precipitation or chemical reaction driven scale growth rate and fluid velocity [14].

In regime B, for fluid velocity higher than 0.1 m/s, the chemical reaction rate may commence to control the overall rate of scaling as increasing fluid velocity does not affect the overall rate of scale growth. On the other hand, when chemical reaction is comparatively fast, the rate of scale growth continuously increases with increasing fluid velocity. In regime C, the rate of scale growth progressively decreases with increase in fluid velocity. In this regime, an increase in fluid velocity results in more erosion, which slows down the scale growth. In regime D, the material surface suffers net loss owing to the effect of erosion more than scale growth.

There are many factors and parameters which contribute to the scale formation and deposition. These are the quality of the bauxite ore (concentration of silica and other impurities in bauxite), the saturation level of caustic solution, the rheological properties (viscosity, temperature and density), the process equipment (material, surface finish and morphology), the turbulence and inertia of suspended particles, the velocity (stream-wise, cross-stream and circumferential velocity fluctuation components) of fluid particles, the particle size and shape and the adhesive property of the particles.

The scale formation mechanism in the Bayer process equipment is still not well understood. Most of the above parameters are related to fluid dynamics characteristics of the Bayer liquor and play a critical role in scale formation. It is important to discern the scale formation mechanism before attempting to optimise efforts to suppress the scale growth. Reduction of scale has remained a challenge and detailed research is needed to adequately address this critical and

important issue. Furthermore, this research will provide new insight knowledge about the scale growth mechanism and factors involved in reducing scale on the process equipment through fluid dynamics design.

Fundamentals of scaling

Historically, interaction of particles with turbulent flow is characterised by the dimensionless particle relaxation time, which is the ratio of the particle relaxation time τ_p to the time scale of near-wall turbulent structures. The dimensionless particle relaxation time [19] based on Stokes drag law is defined as:

$$\tau_p = \frac{\rho_p d_p^2}{18\rho_f \nu_f} \quad (1)$$

The Kolmogorov time scale of fluctuations based on volume-averaged viscous energy dissipation is [20]:

$$\tau_e = \frac{\nu_f}{(u*)^2} \quad (2)$$

where $u*$ is the friction velocity defined as:

$$u* = \sqrt{\frac{\tau_w}{\rho_f}} \quad (3)$$

where τ_w is the wall shear stress.

For a symmetrical developed pipe flow, when the wall shear stress at a pipe surface is uniform, the friction velocity may be expressed as a function of the average velocity and the friction factor *f* as:

$$u* = U_0\sqrt{\frac{f}{8}} \quad (4)$$

The particle relaxation time τ_p^+ for a pipe flow yields from the combination of Eqs. (1) - (4) as:

$$\tau_p^+ = \frac{\tau_p}{\tau_e} = \frac{\rho_p d_p^2 U_0^2 f}{144\rho_f \nu_f^2} \quad (5)$$

The behaviour of the interaction of particles with turbulent flow is highly dependent on the value of their dimensionless relaxation time. If τ^+_p is very small, particles have the ability to closely follow all the turbulent fluctuations of a fluid. At larger values of τ^+_p, the trajectories of particles and their velocity deviate from the fluid particles' path. Large particles are only slightly affected by small eddies, and respond mainly to the larger eddies which usually occur at greater distances from the wall.

TARGET MODEL

The full-scale concentric reducer was numerically modelled in this study as shown in Figure 2. The rate of contraction of the cross-sectional area of the reducer along its axis was not uniform. The rate of area reduction between sections A-A and B-B gradually increases and reaches its maximum rate near the section B-B as shown in Figure 3. This maximal reduction rate remained virtually constant throughout the sections C-C and D-D, before gradually decreasing when approaching section E-E and then diminished to zero at section F-F. The rate of strain imposed on the flowing water could affect the behaviour of the fluctuating velocity.

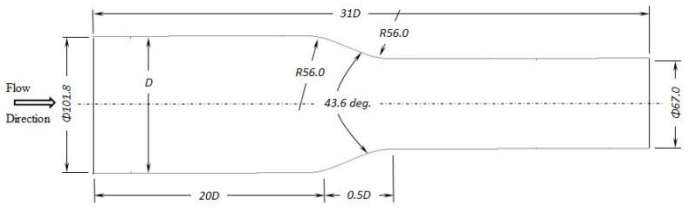

Figure 2 Schematic diagram of full-scale concentric reducer.

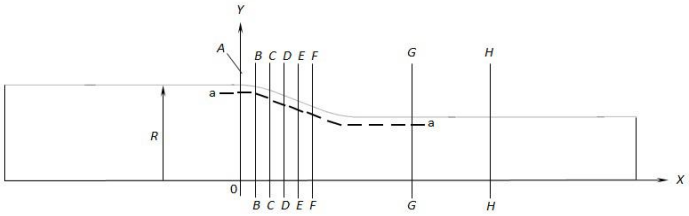

Figure 3 Symmetric half section of concentric reducer positions of the sections where the stream-wise and cross-stream velocity components were measured.

The stream-wise u'_x and cross-stream u'_r components of the instantaneous velocities were measured along several sections through: A-A to G-G as shown in Figure 3. Section A-A was positioned at the boundary between the end of the straight pipe and entrance to the reducer. The five sections B-B to F-F were separated from section A-A and from each other by the uniform distance of 8 mm. The last sections G-G and H-H were located within the smaller straight pipe at a distance of 36 mm and of 86 from F-F, respectively.

NUMERICAL METHOD

The governing equations being solved in Reynolds stress model (RSM) are continuity, momentum and turbulence equations by commercial CFD code ANSYS (FLUENT) version 15.0. For an incompressible fluid, the equations of continuity and momentum balance for the mean motion are given as:

$$\frac{\partial \bar{u}_i}{\partial x_i} = 0 \quad (6)$$

$$\frac{\partial \bar{u}_i}{\partial t} + \bar{u}_j \frac{\partial \bar{u}_i}{\partial x_j} = -\frac{1}{\rho}\frac{\partial \bar{p}}{\partial x_i} + \nu \frac{\partial^2 \bar{u}_i}{\partial x_j \partial x_j} - \frac{\partial}{\partial x_j} R_{ij} \quad (7)$$

where $R_{ij} = \overline{u'_i u'_j}$ is the Reynolds stress tensor and $u'_i = u_i - \bar{u}_i$

The Reynolds stress model (RSM) involves calculation of the individual turbulence stresses via a differential transport equation given as:

$$\underbrace{\frac{\partial}{\partial t}R_{ij}+\bar{u}_k\frac{\partial}{\partial x_j}R_{ij}}_{\text{convective transport}}=\underbrace{+\frac{\partial}{\partial x_k}\left(\frac{\nu_t}{\sigma^k}\frac{\partial}{\partial x_k}R_{ij}\right)}_{\text{diffusive transport}}$$
$$\underbrace{-\left[\overline{u_i'u_k'}\frac{\partial\bar{u}_j}{\partial x_k}+\overline{u_j'u_k'}\frac{\partial\bar{u}_i}{\partial x_k}\right]}_{P_{ij}=\text{production}} \quad (8)$$
$$\underbrace{-C_1\frac{\varepsilon}{\kappa}\left[R_{ij}-\frac{2}{3}\delta_{ij}\kappa\right]-C_2\left[P_{ij}-\frac{2}{3}\delta_{ij}P\right]}_{\phi_{ij}=\text{pressure strain}}-\underbrace{\frac{2}{3}\delta_{ij}\varepsilon}_{\varepsilon_{ij}=\text{dissipation}}$$

The governing equations were discretised by using the vertex-centered finite volume method. The second-order central differencing scheme was applied for the spatial derivatives of the pressure term and the second-order upwind scheme was used for the momentum term. The specific dissipation rate and Reynolds stresses were discretised using the first-order upwind scheme. Pressure-velocity coupling was preserved by using the Coupled algorithm.

Grid Independence Test

For the grid independence study, the working fluid has been taken as water and the simulation was run for Re = 27,130 and 43,740 based on an inlet diameter (D=101.8 mm) and two velocities (U_0 = 0.268 m/s and 0.432 m/s, respectively). Grid independence tests were carried out to find out the optimum grid size for the numerical study.

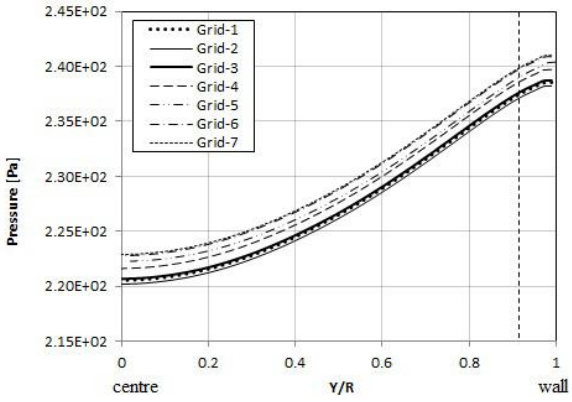

Figure 4 Comparison of pressure distribution for different grid size at Re = 27,130.

Seven different grid sizes (250×80, 400×90, 600×110, 900×150, 1200×200, 1200×250 and 1200×270 termed Grid-1, Grid-2, Grid-3, Grid-4, Grid-5, Grid-6, and Grid-7, respectively) were tested to determine the effect on the pressure distribution calculated at section B (as shown in Figure 4) from the centre to the wall. It was found that there was no significant change in pressure distribution beyond the grid size of 1200×250 (300,000 as Grid-6). Therefore, for the numerical simulation, the grid size of 300,000 has been used to perform all the simulations.

Validation of Numerical Models

The problem-specific numerical model was validated numerically with the use of the commercially available computational package, ANSYS (Fluent). An experimental PIV results for Re = 40,000 is presented in Figure 5 which was conducted in our lab previously. A comparison of the velocity vector distributions obtained for the same Reynolds number and the same fluid as water from the ANSYS simulation is shown in **Error! Reference source not found.**6. It was found that the two-dimensional model predicted relatively good agreement.

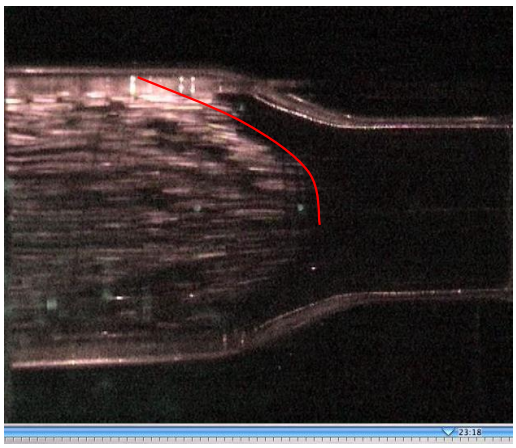

Figure 5 Experimental results of Re = 40,000 with water.

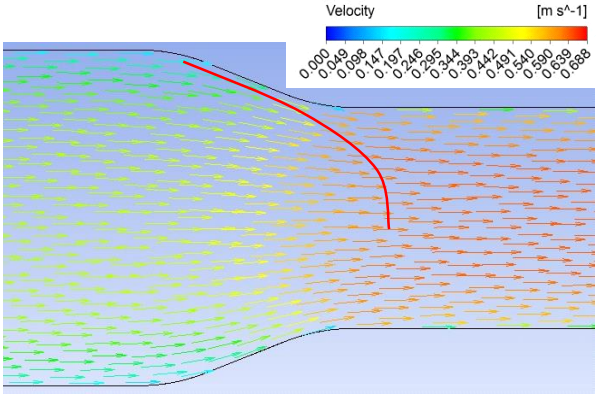

Figure 6 Numerical results of Re = 40,000 with water.

RESULTS AND DISCUSSION

The variation of both stream-wise u'_x and cross-stream u'_r fluctuating velocity components along the reducer model were measured at a distance of 0.08R from its wall. The results are presented in Figure 7 and Figure 8 in the form of the RMS value of a respective fluctuating velocity component related to the mean in the 101.8 mm diameter pipe versus the distance from the section A-A measured along the axis of the reducer in the direction of flow.

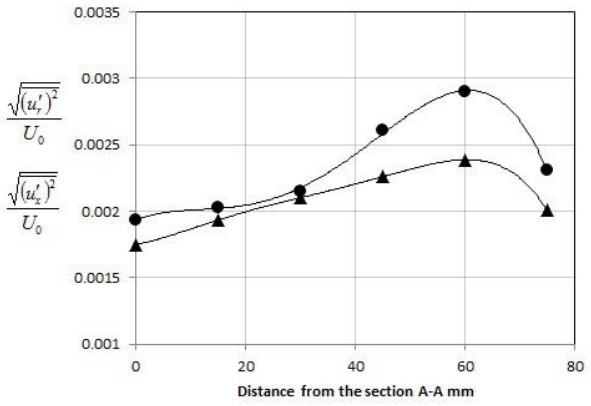

Figure 7 Variations of normalised fluctuating components $\sqrt{\overline{(u_r')^2}}/U_0$ (●) and $\sqrt{\overline{(u_x')^2}}/U_0$ (▲) along the X-axis at the distance of 0.08R from the internal surface of the reducer: Re = 27,130 and V=0.268 m/s (101.8 mmϕ pipe).

The stream-wise (u_x') and cross-stream (u_r') fluctuating velocity components exhibit the following trends (as shown in Figure 7) as flow passes through the concentric reducer. For both Reynolds numbers, the stream-wise fluctuating component shows only a slight variation at the entry to the reducer, however, it then increases more in the section between D-D to F-F. When the rate of contraction starts diminishing near the section F-F, the component u_x' shows a decrease for the inlet velocity of 0.268 m/s, and a sharp decrease for the inlet velocity of 0.432 m/s. The overall increase of u_x' did not exceed 18% of its value at the entry to the reducer.

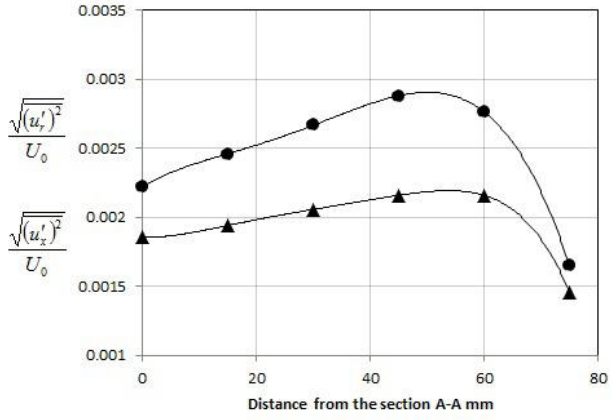

Figure 8 Variations of normalised fluctuating components $\sqrt{\overline{(u_r')^2}}/U_0$ (●) and $\sqrt{\overline{(u_x')^2}}/U_0$ (▲) along the X-axis at the distance of 0.08R from the internal surface of the reducer: Re = 43,740 and V=0.432 m/s (101.8 mmφ pipe).

The cross-stream fluctuating velocity component u_r' reveals a remarkable increase between B-B to E-E and starts decreasing sharply after passing F-F. The cross-stream fluctuating velocity component u_r' increases about 2-fold for the lower velocity and about 1.5 fold for the higher velocity.

As we discern from the theory, the value of the cross-stream fluctuating velocity component u_r' outside of the boundary layer is dominating parameters determining the deposition rate of particles suspended in the flowing fluid. The gradient of u_r' pointing towards the solid surface determines both the rate of turbulent diffusion and the rate of turbophoresis for the particles depositing in the diffusion-impaction regime. It is ascertained that the increase of cross-stream fluctuating velocity component in the reducer has a strong influence to promote scale growth on the wall. In contrast, an increase in the stream-wise fluctuating velocity component is less pronounced but it accelerates the erosion of the deposited scale on the wall.

CONCLUSION

A numerical study has been performed to assess the variation of fluctuating velocity components of water flow through the concentric reducer. The cross-stream, u_r' fluctuating velocity component in the reducer is greater than the stream-wise u_x' fluctuating velocity component in the reducer; it is believed that this is one of the reasons for more particle deposition as well as more scale growth in the concentric reducer. In contrast, the stream-wise u_x' fluctuating velocity component is responsible for erosion of deposited particles from the solid wall.

REFERENCES

[1] S. J. Nawrath, M. M. K. Khan, and M. C. Welsh, "An experimental study of scale growth rate and flow velocity of a super-saturated caustic–aluminate solution," *International Journal of Mineral Processing*, vol. 80, pp. 116-125, 9// 2006.

[2] D. Thomas, "Swirl Flow Agitation- QAL/CSIRO Collaborative Research Program 2000," *Presentation to Queensland Alumina Limited Technical Advisory Committee- April.*, 2000.

[3] H. Yu, R. Sheikholeslami, and W. O. S. Doherty, "Mechanisms, thermodynamics and kinetics of composite fouling of calcium oxalate and amorphous silica in sugar mill evaporators—A preliminary study," *Chemical Engineering Science*, vol. 57, pp. 1969-1978, 6// 2002.

[4] E. Neofotistou and K. D. Demadis, "Use of antiscalants for mitigation of silica (SiO2) fouling and deposition: fundamentals and applications in desalination systems," *Desalination*, vol. 167, pp. 257-272, 8/15/ 2004.

[5] F. Coletti and S. Macchietto, "A dynamic, distributed model of shell-and-tube heat exchangers undergoing crude oil fouling," *Industrial & Engineering Chemistry Research*, vol. 50, pp. 4515-4533, 2011.

[6] M. Loan, C. Klauber, and C. Vernon, "A fundamental study of gibbsite scale nucleation on mild steel," in *Proceedings of the 8th International Alumina Quality Workshop, Darwin, Australia*, 2008, pp. 334-339.

[7] T. A. Hoang, M. Ang, and A. L. Rohl, "Effects of Process Parameters on Gypsum Scale Formation in Pipes," *Chemical Engineering & Technology*, vol. 34, pp. 1003-1009, 2011.
[8] X. Xiaokai, M. Chongfang, and Y. C., "Mechanism of Calcium Carbonate Scale Deposition under Subcooled Flow Boiling Conditions," *Chinese Journal of Chemical Engineering*, vol. 13, pp. 464-470, 2005.
[9] S. Ibrahim and A. Nienow, "Particle suspension in the turbulent regime: the effect of impeller type and impeller/vessel configuration," *Chemical engineering research & design*, vol. 74, pp. 679-688, 1996.
[10] A. Nienow, "The suspension of solid particles," *Mixing in the process industries*, vol. 2, 1997.
[11] J. Wu, Y. Zhu, and L. Pullum, "Impeller geometry effect on velocity and solids suspension," *Chemical Engineering Research and Design*, vol. 79, pp. 989-997, 2001.
[12] C. M. Chapman, A. Nienow, M. Cooke, and J. Middleton, "Particle-gas-liquid mixing in stirred vessels. I: Particle-liquid mixing," *Chemical engineering research and design*, vol. 61, pp. 71-81, 1983.
[13] J. Wu, L. J. Graham, and N. Noui-Mehidi, "Intensification of mixing," *Journal of Chemical Engineering of Japan*, vol. 40, pp. 890-895, 2007.
[14] J. Wu, G. Lane, I. Livk, B. Nguyen, L. Graham, D. Stegink, *et al.*, "Swirl flow agitation for scale suppression," *International Journal of Mineral Processing*, vol. 112–113, pp. 19-29, 9/10/ 2012.
[15] J. Wu, L. J. Graham, and N. Noui Mehidi, "Estimation of agitator flow shear rate," *AIChE journal*, vol. 52, pp. 2323-2332, 2006.
[16] J. Wu, S. Wang, L. Graham, R. Parthasarathy, and B. Nguyen, "High solids concentration agitation for minerals process intensification," *AIChE Journal*, vol. 57, pp. 2316-2324, 2011.
[17] J. Wu, Y. G. Zhu, and L. Pullum, "Suspension of high concentration slurry," *AIChE Journal*, vol. 48, pp. 1349-1352, 2002.
[18] J. Wu, B. Nguyen, and L. Graham, "Energy efficient high solids loading agitation for the mineral industry," *The Canadian Journal of Chemical Engineering*, vol. 88, pp. 287-294, 2010.
[19] A. V. Deev, T. Rasheed, M. C. Welsh, M. M. K. Khan, and M. G. Rasul, "Measurement of instantaneous flow velocities in a concentric reducer using Particle Image Velocimetry: Study of scale deposition," *Experimental Thermal and Fluid Science*, vol. 33, pp. 1003-1011, 9// 2009.
[20] C. Marchioli, A. Giusti, M. Vittoria Salvetti, and A. Soldati, "Direct numerical simulation of particle wall transfer and deposition in upward turbulent pipe flow," *International Journal of Multiphase Flow*, vol. 29, pp. 1017-1038, 6// 2003.